Polymer-Dispersed Liquid Crystals with Co-continuous Structures Generated by Polymerization-Induced Phase Separation of EBBA−Epoxy Solutions

C. E. Hoppe, M. J. Galante, P. A. Oyanguren, and R. J. J. Williams*

Institute of Materials Science and Technology (INTEMA), University of Mar del Plata−National Research Council (CONICET), J. B. Justo 4302, 7600 Mar del Plata, Argentina

Received January 7, 2002

ABSTRACT: Polymer-dispersed liquid crystals (PDLCs), consisting of a dispersion of LC-rich domains in a polymer matrix, are used in different types of electrooptical devices. Their efficiency can in principle be increased if the LC domains exhibit a uniform characteristic size in the range of the wavelength of visible light. In an attempt to generate this type of morphology, a model PDLC system based on a 50 wt % solution of *N*-4-ethoxybenzylidene-4′-*n*-butylaniline (EBBA) in an epoxy monomer (diglycidyl ether of bisphenol A, DGEBA) was analyzed. The polymerization-induced phase separation was performed at 80 °C, using a tertiary amine as initiator (benzyldimethylamine, BDMA). By selecting an initial concentration located close to the critical composition to promote spinodal demixing, co-continuous morphologies were obtained, which were rapidly fixed by gelation. The conversion of epoxy groups (p) was followed by near-infrared spectroscopy (NIR). At $p = 0.28$, phase separation took place as revealed by transmission optical microscopy (TOM) and by the acceleration observed in the isothermal cure rate. Gelation took place at $p = 0.35$, soon after the cloud point. Although the primary structure was arrested by gelation, the LC-rich phase was continuously enriched in pure EBBA, as revealed by the increase in T_{NI} with conversion monitored by differential scanning calorimetry (DSC). Co-continuous structures remained unmodified after the storage of PDLCs for several months. The nematic range of the LC-rich phase at $p = 1$ was comprised between 34 °C (melting point) and $T_{NI} = 68$ °C. A 57% of the initial LC was present in nematic domains at 40 °C, as determined by the variation of the FTIR absorbance of a characteristic LC peak between isotropic and nematic states. Therefore, a possible route to obtain PDLCs with a uniform characteristic size of LC domains is to start with a composition close to the critical one and select conditions to produce liquid−liquid demixing soon before gelation.

Introduction

Polymer-dispersed liquid crystals (PDLCs), consisting of a dispersion of LC-rich domains in a polymer matrix, are potential materials for electrooptical devices such as reflective displays, optical switches, and variable transmittance windows.[1−4] They can be electrically switched between a strongly scattering state and a highly transparent state. The contrast ratio, switching voltage, switching speed, and hysteresis are mainly determined by the morphologies and compositions of both phases. LC domains with sizes much smaller than the wavelength of visible light do not scatter light efficiently; domain sizes much larger than the wavelength of visible light lead to a poor contrast ratio. Therefore, it is desirable to generate LC domains with a uniform characteristic size in the wavelength range of visible light. It has been suggested that co-continuous morphologies generated by liquid−liquid spinodal demixing in the course of polymerization should exhibit the desired uniform characteristic size of LC domains.[5] The aim of this study is to explore this possibility using a model system based on a single liquid crystal and thermoset precursors with a relatively simple polymerization chemistry.

N-4-Ethoxybenzylidene-4′-*n*-butylaniline (EBBA) was selected as liquid crystal (Figure 1). According to the literature,[6−9] the temperature range where the nematic phase of EBBA is stable lies in the range comprised from about 36 °C (T_m: melting temperature) to about 77 °C

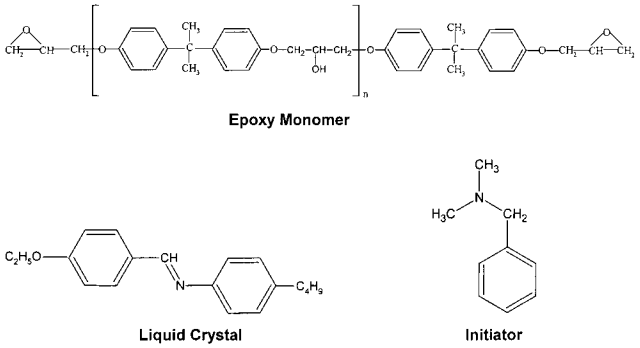

Figure 1. Chemical structures of liquid crystal (EBBA), epoxy monomer (DGEBA), and initiator (BDMA).

(T_{NI}: nematic−isotropic transition temperature). Reported values of T_m and T_{NI} vary in a range of a few degrees around these values. Although crystallization of EBBA prevents its use in a PDLC operating at room temperature, it was selected to avoid the fractionation problems present in eutectic mixtures employed in commercial formulations. Several metastable crystal structures are known for EBBA.[6,7,9−12] Although a glass transition temperature corresponding to a supercooled nematic state was reported ($T_g = -54$ °C),[7] this state could not be found by other authors, even when employing very fast cooling rates.[9] Phase diagrams of binary solutions of aromatic hydrocarbons,[13] polystyrene and poly(ethylene oxide)[14−16] in EBBA, have been reported. However, to our knowledge, EBBA has not been used to generate PDLCs by polymerization-induced phase separation (PIPS).

* To whom correspondence should be addressed.

10.1021/ma0200120 CCC: $22.00
Published on Web 06/29/2002

Usual thermoset precursors to generate PDLCs by PIPS are mixtures of UV-curable multifunctional monomers, including a photoinitiator.[17−27] These systems have the advantage that they permit to select independently the curing temperature and the rate of polymerization. Therefore, thermodynamics and kinetics may be decoupled. However, the analysis of the phase separation process in the course of the fast polymerization requires the use of relatively sophisticated experimental techniques (real-time FTIR spectroscopy can provide valuable information[23,24]). In this study, we selected an epoxy monomer (diglycidyl ether of bisphenol A, DGEBA) as thermoset precursor (Figure 1). In the presence of a tertiary amine as initiator (benzyldimethylamine, BDMA, Figure 1), DGEBA undergoes an anionic polymerization at a relatively slow polymerization rate, leading to a polymer network.[28] The reaction proceeds through a living chainwise mechanism leading to very short primary chains (2−5 epoxy units), due to the high ratio of chain transfer/chain propagation rates.[29−32] Gelation takes place at advanced conversions that depend on the initial concentration of initiator and cure temperature.[33] This favors the possibility of producing phase separation previous to the gel formation.

The strategy used to produce co-continuous structures was to perform the polymerization in the isotropic region of the phase diagram, employing an EBBA concentration located in the critical composition range. In these conditions, a liquid−liquid spinodal demixing mechanism should be favored.[34,35] The next step was to search convenient values of reaction temperature and initiator concentration to produce gelation soon after the beginning of the phase separation process. In this way, if co-continuous structures were produced, they should be fixed by gelation of the polymer network (although mass transfer between phases should occur continuously during the postgel stage). A 50 wt % solution of EBBA was the selected composition for this study. This value is very close to the critical composition predicted by the Flory−Huggins equation before the start of polymerization. Although at the cloud-point conversion the critical point is shifted to higher EBBA concentrations,[36] the predicted shift is small enough to keep the system in the critical concentration region.[35]

A second aim of this study was to analyze the evolution of parameters related to the composition of both phases in the course of the phase separation process. The conversion of epoxy groups at the selected reaction temperature was followed by near-infrared spectroscopy.[37−39] The increase in the glass transition temperature (T_g) of the epoxy-rich phase and the nematic−isotropic transition temperature (T_{NI}) of the LC-rich phase, measured by differential scanning calorimetry (DSC), were used to monitor the evolution of both phases after the cloud-point conversion.[40] The fraction of LC that was present in nematic domains at full conversion was determined by FTIR spectroscopy.[24] Finally, the evolution of the system during polymerization was visualized using a phase-transformation diagram similar to the one described by Boots et al.[41]

Experimental Section

Materials. The chemical structures of liquid crystal, epoxy monomer, and initiator are shown in Figure 1. The liquid crystal *N*-4-ethoxybenzylidene-4′-*n*-butylaniline (EBBA, Aldrich, 98% purity) was used as received. The epoxy monomer, based on diglycidyl ether of bisphenol A (DGEBA, MY790 Ciba), had an epoxy equivalent weight of 174 g/mol. The initiator of the epoxy polymerization was benzyldimethylamine (BDMA, Aldrich), in an amount of 0.06 mol of BDMA per mole of epoxy groups. EBBA and DGEBA were mixed in the desired proportions at 50 °C, and the solution was cooled to room temperature where the appropriate BDMA amount was added. Most of the study was performed with a 50 wt % solution of EBBA in the mixture with DGEBA and BDMA.

Techniques. Differential scanning calorimetry (DSC, Pyris 1, Perkin-Elmer) was used to determine the temperatures of various transitions occurring in both phases: crystallization (T_K) and melting temperatures (T_m) of EBBA, nematic−isotropic transition temperature (T_{NI}) of the EBBA-rich phase, and glass transition temperature (T_g) of the epoxy-rich phase. These temperatures were determined during a heating scan at 10 °C/min under nitrogen, following a cooling scan at the same rate. Both T_m and T_{NI} were measured at the end of the corresponding transition, and T_g was taken at the onset of the glass transition (T_K values were not analyzed). For binary EBBA−DGEBA solutions devoid of initiator, T_{NI} values were also determined by placing a test tube containing the corresponding solution in a thermostat and finding the clearing temperature during a heating scan by visual inspection. Temperature was increased in small steps, keeping it constant for some minutes at each one of the steps. T_{NI} was defined as the temperature at which the solution became completely homogeneous.

Transmission optical microscopy (TOM) was employed to determine the cloud-point time in the course of polymerization (liquid−liquid phase demixing) and to follow the evolution of generated morphologies. A Leica DMLB microscope provided with a video camera (Leica DC 100) and a hot stage (Linkam THMS 600), was used for these purposes. Samples were placed between two glasses using a 0.5 mm stainless steel spacer. To obtain optical micrographs of final morphologies with a good contrast, PDLCs were prepared as coatings on glass surfaces. They were cured in an oven at 80 °C for 24 h, cooled, and stored at room temperature or −18 °C for different periods of time (the storage at −18 °C promoted a fast crystallization of EBBA). After cure, some of the coated glasses were treated with 2-propanol at 60 °C, until complete elimination of the EBBA-rich phase as revealed by the transparency of the resultant materials. After a particular storage period (from several hours to several months), both the untreated and the 2-propanol-treated coatings were placed in the hot stage, heated to a temperature above T_{NI}, and cooled to the desired temperature. Micrographs were taken with and without crossed polarizers.

The time to gel at 80 °C was determined from solubility tests in tetrahydrofuran (THF). Test tubes containing the 50 wt % EBBA formulation were placed in a thermostat at 80 °C. Each one of them was extracted from the thermostat at different times, and the solubility of the partially reacted material in THF was observed. The presence of a gel was evidenced when a fraction of the initial sample remained in a swollen state at the bottom of the tube. A series of runs were performed to obtain a better precision of the time at which the first appearance of a gel fraction could be evidenced by visual inspection.

Near-infrared spectroscopy (NIR) was used to determine the polymerization kinetics of both the neat epoxy and solutions with 50 wt % EBBA. An FTIR (Genesis II, Mattson), provided with a heated transmission cell (HT-32, Spectra Tech) with quartz windows (32 mm diameter) and a programmable temperature controller (Omega, Spectra Tech, $\Delta T = \pm 1$ °C), was employed. The sample was placed in a polyethylene bag inserted between the quartz windows. (Polyethylene did not exhibit absorption peaks in the spectral range of interest.) The reaction was carried out at 80 °C, following the height of the absorption band at 4530 cm^{-1} (assigned to the conjugated epoxy CH_2 deformation band with the aromatic CH fundamental stretch),[39] with respect to the height of a reference band at 4621 cm^{-1} (assigned to a combination band of the aromatic conjugated C═C stretch with the aromatic CH

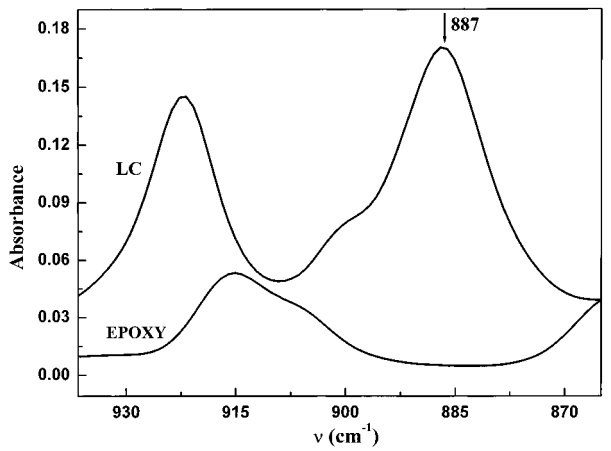

Figure 2. FTIR absorption bands of EBBA (LC) and DGEBA (epoxy) in the range of 870−930 cm^{-1}.

fundamental stretch).[39] The final thickness of the cured film was 2.3 mm.

FTIR spectroscopy was also used to determine the fraction of EBBA present in nematic domains in the fully cured material. As discussed by Bhargava et al.,[24] nematic ordering can be quantified by the change in the absorbance of a characteristic band of the LC between isotropic and nematic states. Among the EBBA bands that exhibited this behavior, the peak at 887 cm^{-1} (possibly arising from vibrations involving in-phase C−C−C stretch mixed with in-plane CH_3 rock)[42] was selected because no overlapping with DGEBA bands was observed in this region (Figure 2). A drop of EBBA was placed between two KBr windows, and the FTIR spectra were recorded at 85 °C (isotropic state) and at 40 °C (nematic state). The absorbance of a set of peaks remained constant, meaning that there had not been any significant change of the sample thickness. Another set of peaks exhibited a change in the absorbance at 40 °C with respect to the one at 85 °C. For the peak at 887 cm^{-1}, the relative change of the absorbance was

$$[A_{EBBA}(40\ °C) - A_{EBBA}(85\ °C)]/A_{EBBA}(85\ °C) = 0.130 \quad (1)$$

This change corresponds to a 100% fraction of the LC in the nematic state. A similar ratio was determined for the fully cured PDLC to estimate the fraction of EBBA present in nematic domains at 40 °C. A drop of the initial formulation containing 50 wt % EBBA was cured between two KBr windows at 80 °C for 24 h. The fraction of EBBA in nematic domains was calculated by

$$(1/0.130)[A_{PDLC}(40\ °C) - A_{PDLC}(85\ °C)]/A_{PDLC}(85\ °C) \quad (2)$$

Results and Discussion

DGEBA−EBBA Phase Diagram. The phase diagram of the binary DGEBA−EBBA solution devoid of initiator was first determined (Figure 3). One-phase regions (I, N, K) and regions of coexistence of two phases (I + N, N + K, I + K) are indicated. No isotropic−isotropic coexistence region was found, indicating the high initial solubility of both components before the start of polymerization. T_m values were determined from DSC scans at 10 °C/min, and T_{NI} values were measured by visual inspection: appearance of a homogeneous solution in the course of a very slow heating scan or obtained from DSC scans. The dashed line giving the boundary of nematic domains was predicted theoretically, as discussed below. The phase diagram is completely analogous to the one reported by Shaya and Yu[43] for a biphenyl−MBBA system. (MBBA has a chemical structure similar to EBBA, with a methoxy instead of an ethoxy group.)

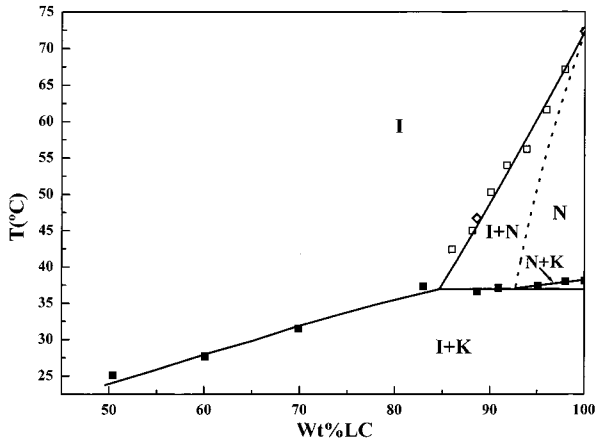

Figure 3. Phase diagram of the EBBA−DGEBA binary system showing one-phase regions (I, N, K) and regions of coexistence of two phases (I + N, N + K, I + K). T_m values (■) were determined from DSC scans at 10 °C/min; T_{NI} values were measured by visual inspection: appearance of a homogeneous solution in the course of a very slow heating scan (□) or obtained from DSC scans (◇). The dashed line representing the boundary of the nematic phase was predicted from the Flory−Huggins−Maier−Saupe model.

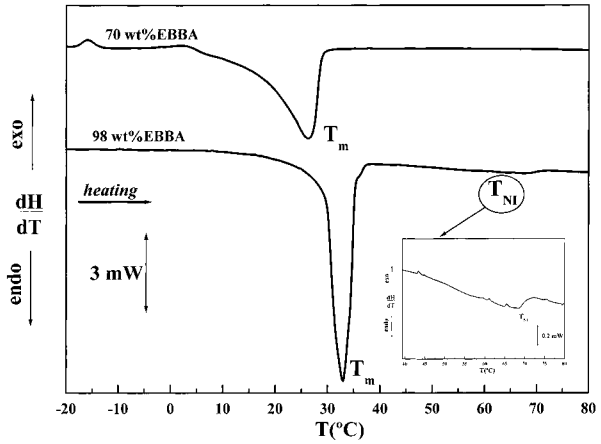

Figure 4. DSC thermograms obtained during a heating scan at 10 °C/min for DGEBA−EBBA solutions containing 70 wt % EBBA and 98 wt % EBBA. The inset shows a magnification in the region of the nematic−isotropic transition.

The nematic−isotropic transition temperature of EBBA was T_{NI} = 73 °C, a few degrees lower than literature values possibly because of impurities present in the commercial product. Its melting temperature was T_m = 38 °C, in agreement with values reported in the literature.[6,9] As results from the phase diagram, T_{NI} is much more affected by impurities than T_m. The straight line joining T_m of EBBA with the intersection of the calculated dashed line and the horizontal at 37 °C gives the upper boundary of the coexistence of nematic and crystalline phases. The observed T_m depression was about 1 °C for DGEBA−EBBA, much less than the 5 °C found for the biphenyl−MBBA system.[43]

Examples of DSC thermograms are shown in Figure 4 for solutions containing 70 and 98 wt % EBBA. The exothermic peak preceding melting for the sample containing 70 wt % EBBA is due to the additional crystallization produced during the heating scan. The melting peak is extended in a relatively broad temperature range. This is due to the continuous melting of crystals required to establish equilibrium when increasing temperature at a constant composition in the I + K

coexistence region. For EBBA concentrations lower than 85 wt %, no nematic−isotropic transition was observed in DSC thermograms. For higher EBBA concentrations, a broad peak of low intensity was observed due to the nematic−isotropic transition taking place for a solution evolving through the corresponding coexistence region. The end of any of these transitions was assigned to a point located in the boundary of the particular coexistence region.

The boundaries of the nematic−isotropic coexistence region may be theoretically calculated using the Flory−Huggins theory for the free energy of mixing of isotropic phases in conjunction with the Maier−Saupe theory for phase transition of a nematic liquid crystal.[44,45] Details of these calculations may be found in the literature.[16,36,46] What is needed is the relationship of the Flory−Huggins interaction parameter (χ), with temperature, usually written in the form $\chi = a + b/T$, with $b > 0$ (upper critical solution temperature behavior). Otherwise, the $\chi(T)$ relationship can be obtained from the best fitting of the theory with the experimental data. However, in our system the nematic−isotropic transition region is limited by the formation of a crystalline phase. In the restricted temperature range where the theory could be fitted to the experimental data, any $\chi(T)$ relationship giving values comprised between 0 and 1 provided a reasonable fitting. The boundaries of the nematic−isotropic coexistence region shown in Figure 3 (continuous and dashed lines) were calculated using $\chi = 0.5$. (Curves for $\chi = 0$ and $\chi = 1$ or any $\chi(T)$ relationship giving χ values in the 0−1 range, produced a small shift of these curves comprised within the experimental error range.) Therefore, the theory was found adequate to fit the experimental external boundary and, consequently, to predict the location of the internal boundary. However, the $\chi(T)$ relationship could not be obtained from this fitting.

The critical composition of the binary DGEBA−EBBA solution was calculated with the Flory−Huggins theory and the knowledge of molar volumes of both components ($V_{DGEBA} = 298$ cm^3/mol, $V_{EBBA} = 279.3$ cm^3/mol). This led to a critical volume fraction of EBBA equal to 0.508 or to a corresponding mass concentration equal to 47 wt % EBBA. When these binary mixtures are subjected to polymerization in the presence of a small amount of initiator, the critical composition is moderately shifted to higher mass fractions of EBBA, following the increase of the average molar volume of the polymerizable component.[35]

Reactive solutions were polymerized at 80 °C, a temperature located above the maximum T_{NI} of the system, to produce an isotropic−isotropic phase separation induced by polymerization. To favor the possibility of generating co-continuous structures through spinodal demixing, an initial EBBA concentration of 50 wt % was selected to produce phase separation in the critical composition range.

Conversion vs Time Curves at 80 °C. Kinetic results obtained from NIR spectra are shown in Figure 5 for both the neat epoxy system and the solution containing 50 wt % EBBA. While for the neat epoxy system the maximum conversion was limited by vitrification ($T_g = 85$ °C for the neat epoxy cured to complete conversion), for the EBBA-modified epoxy, an almost complete conversion could be attained after 24 h, within the experimental error of NIR spectroscopy. This was due to the plasticization effect produced by the LC that remained dissolved in the matrix at complete conversion.

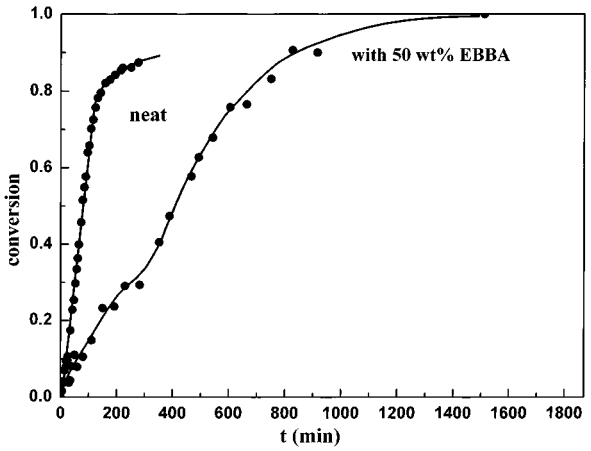

Figure 5. Conversion vs time curves at 80 °C, determined by NIR, for the homopolymerization of DGEBA initiated by BDMA (neat system) and for a solution containing 50 wt % EBBA.

The presence of EBBA produced a significant decrease of the polymerization rate. It took about 4 h to get an almost plateau conversion in the neat system and about 24 h for the complete disappearance of epoxy groups in the EBBA-modified system. The kinetic curve of the EBBA-modified epoxy exhibits a discontinuity of the derivative at conversions close to 0.30. The polymerization rate undergoes an acceleration at this conversion, an effect that may be related to the beginning of the phase separation process. The partial segregation of an EBBA-rich phase produced an increase in the monomer concentration in the epoxy-rich phase and a decrease in the concentration of the component that retarded the polymerization. Both factors explain the acceleration observed in the cure rate. A similar phenomenon has been described for thermoplastic-modified epoxies containing a relative high fraction of thermoplastic in the initial formulation.[35,47]

The increase in the reaction rate produced by phase separation constitutes a direct way to determine a cloud-point conversion in PDLCs produced by PIPS. Another simple method was proposed by Barghava et al.,[24] related to the scattering-induced change in the FTIR absorbance spectrum of the sample, produced by the phase separation process. But this requires that the formed domain size is sufficient to scatter IR radiation, a condition that was not fulfilled in our system. In this regard, this is a poorer method to detect phase separation than conventional light transmission or light scattering techniques.[24]

Cloud-Point Time. A direct determination of the cloud point in the polymerization of the 50 wt % EBBA solution at 80 °C was made by TOM. The beginning of a liquid−liquid phase separation was observed at 220 min, corresponding to a cloud-point conversion, $p_{cp} = 0.28$, in very good agreement with the conversion at which the acceleration in the cure rate was observed.

Gel Conversion. The gel time obtained by solubility measurements in THF was transformed into the corresponding conversion using Figure 5. This led to $p_{gel} = 0.35$. Therefore, a liquid−liquid phase separation preceded gelation in the 50 wt % EBBA-modified epoxy.

The gel conversion in ideal chainwise polymerizations may be predicted using Stockmayer's equation.[48] For the

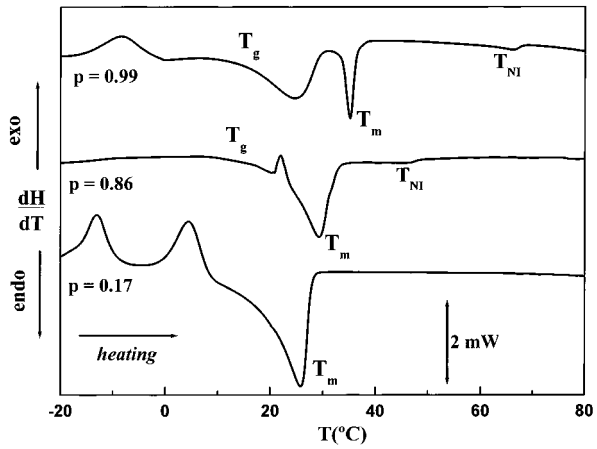

Figure 6. DSC thermograms obtained during heating scans at 10 °C/min, for 50 wt % solutions of EBBA in DGEBA/BDMA, converted to $p = 0.17$, 0.86, and 0.99 at 80 °C.

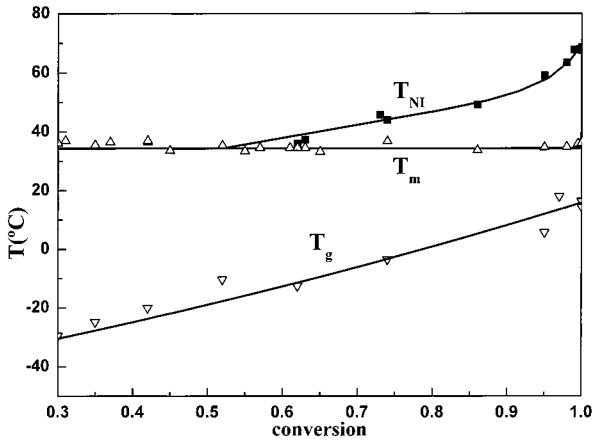

Figure 7. Thermal transitions (T_g of the epoxy-rich phase; T_m and T_{NI} of the EBBA-rich phase) observed in the course of DSC heating scans at 10 °C/min for samples containing 50 wt % EBBA partially cured at 80 °C.

particular case of the homopolymerization of a tetrafunctional monomer, it may be written as

$$p_{gel} = 1/(DP_w - 1) \quad (3)$$

where DP_w is the mass-average degree of polymerization of primary chains. The experimental value of the gel conversion results from $DP_w = 3.86$, which lies in the range of experimental values reported for the homopolymerization of monoepoxides in the presence of tertiary amines.[29−31]

Evolution of Thermal Transitions as a Function of Conversion at 80 °C. Samples of EBBA-modified epoxies (50 wt % of EBBA in a solution with DGEBA/BDMA) were cured in an oven at 80 °C. At predetermined times (related to conversions through Figure 5), samples were extracted from the oven and stored at −18 °C to arrest the polymerization reaction. They were then scanned in the DSC from about −60 to 90 °C at 10 °C/min. Figure 6 illustrates the observed thermal transitions during heating scans for samples previously cured to different conversions.

The sample converted to $p = 0.17$ (before the cloud-point conversion at 80 °C) exhibits two crystallization peaks previous to the broad melting peak. This is due to the presence of several metastable crystalline phases of EBBA.[6,7,9−11] For $p = 0.86$, the glass transition temperature of the epoxy-rich phase (T_g), the melting peak of EBBA (T_m), and the nematic−isotropic transition temperature of the EBBA-rich phase (T_{NI}) are observed. Some crystallization (exothermic peak) occurs simultaneously with melting, a phenomenon that is related to the transformation of metastable crystalline phases. For $p = 0.99$, T_g, T_m, and T_{NI} are observed, together with two crystallization peaks (one at low temperatures and the other one superimposed with the melting peak).

The set of thermal transitions observed in the DSC scans of partially cured samples is plotted in Figure 7 as a function of conversion (for conversions higher than p_{cp}). The glass transition temperature of the epoxy-rich phase (T_g) increased with conversion due to the increase in the cross-link density and to the continuous segregation of LC to the EBBA-rich phase. At full conversion, the epoxy polymer network swollen with EBBA exhibited a T_g equal to 15 °C, indicating the presence of a large plasticization effect (from 85 °C for the neat epoxy to 15 °C for the EBBA-modified epoxy). A stable nematic phase could be found for conversions higher than 0.55. At this particular conversion, the EBBA mass fraction in the LC-rich phase attains the minimum value needed to enter the nematic−isotropic coexistence region. (Figure 3 illustrates this condition for the DGEBA−EBBA binary system.) T_{NI} increased continuously with conversion due to the purification of the EBBA-rich phase in the course of polymerization, in agreement with theoretical predictions.[49] The PDLC reacted to the maximum conversion exhibited a $T_{NI} = 68$ °C, 5 °C lower than the transition of the starting EBBA ($T_{NI} = 73$ °C). As epoxy groups were completely reacted (within the experimental error of NIR spectra), the observed depression in T_{NI} must be ascribed to a fraction of the initiator (BDMA or BDMA−DGEBA adducts) that remains dissolved in the EBBA-rich phase at the end of reaction. The temperature range where a stable nematic phase was present in the final PDLC was comprised between $T_m = 34$ °C and $T_{NI} = 68$ °C. Although T_m values did not exhibit any significant variation with conversion after the cloud point, an increase of T_m with conversion was indeed observed in the 0−0.30 conversion range (not represented in Figure 7).

Residual EBBA Fraction Dissolved in the Epoxy Network. In any PDLC produced by PIPS, a large fraction of the LC is not segregated and remains dissolved in the polymer network at the end of polymerization. A way to reduce the residual liquid crystal solubility in the polymer has been recently described.[22] The determination of the residual fraction is necessary to establish the effectiveness of the phase separation process.

The fraction of initial LC present in nematic domains is usually determined from calorimetric measurements (e.g., from the ratio of the nematic−isotropic transition enthalpy observed in the PDLC with respect to the one of the pure LC).[50,51] For our particular system, this method was not very accurate due to the small value of the nematic−isotropic transition enthalpy of EBBA and the dispersion of values observed in repeated experimental determinations. Therefore, we used the method reported by Barghava et al.,[24] based on the change in the IR absorbance of a characteristic band of the LC between isotropic and nematic states.

As described in the Experimental Section, the particular band of EBBA at 887 cm^{-1} was selected, exhibiting a relative increase in the absorbance of 13.0%

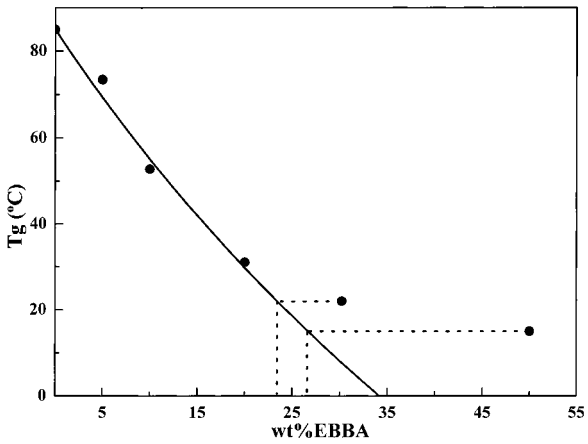

Figure 8. Glass transition temperature of the epoxy network as a function of the wt % EBBA in the initial formulation (onset values determined in a second heating scan at 10 °C/min).

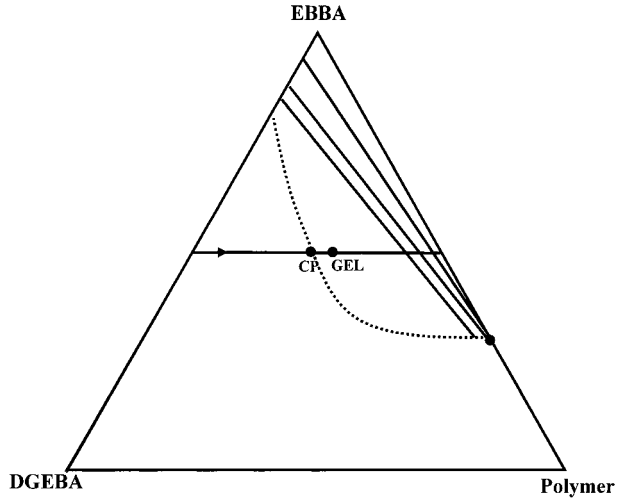

Figure 9. Transformation diagram representing the evolution of the system as a function of conversion.

between isotropic and nematic states (higher absorbance in the nematic state). The change in the relative absorbance of this peak in the fully cured PDLC was 7.4%. This means that the fraction of EBBA present in nematic domains was 7.4/13 = 0.57 of the initial amount. The residual 43% remained dissolved in the epoxy network, giving a mass fraction of EBBA equal to 0.30 (0.43/1.43).

To check this calculation, samples containing 0, 5, 10, 20, 30, and 50 wt % EBBA in the solution with DGEBA/BDMA were cured at 80 °C for 24 h in the hot stage of the transmission optical microscope. Phase separation was only observed for formulations containing 30 and 50 wt % EBBA. Another set of samples was cured in an oven under the same conditions, and glass transition temperatures (T_g) of the cured materials were determined by DSC (onset values obtained in a second heating scan). Figure 8 shows the T_g values of the epoxy network as a function of the wt % EBBA in the initial formulation. Values in the range 0−20 wt % EBBA could be fitted with the Fox equation:[52]

$$1/T_g = w_{LC}/T_{g,LC} + (1 - w_{LC})/T_{g,E} \qquad (4)$$

The glass transition temperature of the liquid crystal, $T_{g,LC}$, is a virtual value corresponding to an isotropic glassy state (a nematic glassy has been reported[7] although its existence has been questioned[9]). By using the experimental value of $T_{g,E}$ (358 K) and taking $T_{g,LC}$ = 187.3 K as a fitting parameter, the curve shown in Figure 8 was plotted. A reasonable fitting resulted for samples that did not exhibit phase separation. The other two samples may be shifted to the curve by assuming that the residual concentration of EBBA is 23.3 wt % for the sample initially containing 30 wt % EBBA and 26.6% for the sample with 50 wt % EBBA. The last value is close to the value estimated from the change in the IR absorbance of a characteristic peak (30 wt %).

However, it is still necessary to explain the observed decrease in T_g for the formulation with 50 wt % EBBA with respect to the one with 30 wt % EBBA. This means that when the polymerization is performed in a more diluted solution (a higher wt % of EBBA), the resulting polymer network is able to dissolve more LC at full conversion. The increase of the swelling capacity may be ascribed to the increase in the concentration of intramolecular cycles with dilution and the corresponding decrease in cross-link density. This can reconcile the fact that polymerizing a 50 wt % EBBA solution led to a residual mass fraction of EBBA in the epoxy equal to 30 wt %, while polymerizing a 30 wt % EBBA solution, under the same conditions, produced phase separation in the course of reaction. As a corollary, it may be stated that the estimation of the residual LC mass fraction in the polymer network, based on experimental measurements for samples containing different LC amounts, has to be made with caution due to the variation of the network topology with dilution.

Transformation Diagram Describing the Phase Separation at 80 °C. The isotropic−isotropic phase separation process taking place at 80 °C may be visualized in a triangular diagram as the one shown in Figure 9.[41] This simplified description of the system is made on the basis of three components: the monomer (DGEBA), the LC (EBBA), and the polymer. This last one is in fact composed of a distribution of species, which are finite in the pregel stage and include one "infinite" species (the gel) in the postgel stage. Therefore, the triangular diagram presented in Figure 9 should not be regarded as a phase diagram. A thermodynamic analysis of the phase separation process must take into account the fractionation of the polymer population between both phases at any conversion in the polymerization reaction.[36,49]

In the simplified description illustrated by Figure 9, the system evolves along the horizontal line located at 50 wt % EBBA, starting in the EBBA−DGEBA side and ending in the EBBA−polymer side at full conversion. For a particular conversion p, the residual fraction of unreacted DGEBA is proportional to $(1 - p)^2$ (simultaneous probability that both epoxy groups of the same molecule remain unreacted, assuming that they react independently). Therefore, the fraction of polymer is $1 - (1 - p)^2$. The cloud point (CP) is located at a DGEBA fraction equal to $(1 - 0.28)^2 = 0.518$, and gelation takes place when the DGEBA fraction is equal to $(1 - 0.35)^2 = 0.422$. Both points are represented along the horizontal trajectory. At full conversion, the system is represented as being composed of pure EBBA (actually the LC-rich phase is contaminated by the initiator or its adducts with DGEBA) and a polymer network with 30 wt % residual EBBA. The dashed envelope traced in a qualitative form encloses the two-phase region. In this simplified analysis it was assumed that the LC-rich

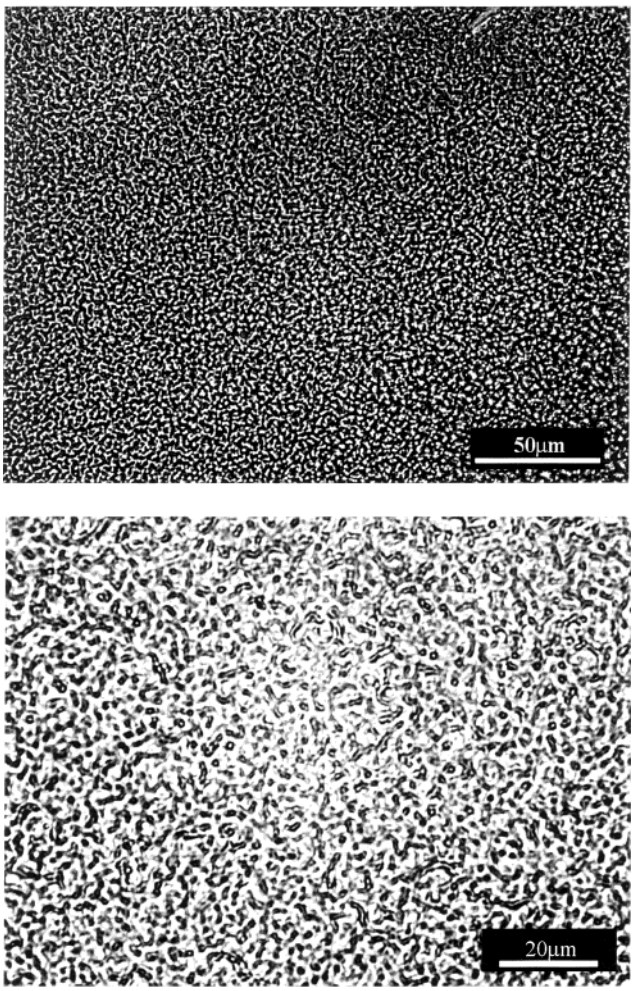

Figure 10. Transmission optical micrographs taken at 40 °C without polarizers, showing co-continuous morphologies generated in the fully reacted material containing 50 wt % EBBA: (a, top) without leaching EBBA; (b, bottom) after leaching EBBA with 2-propanol.

phase only contains DGEBA. In fact, a fractionation of the polymer occurs with other low molar mass species being present in the LC-rich phase. However, the residual monomer is the most significant species fractionated with the LC.[36,49] Tie lines represent the estimated composition of both phases for different particular conversions. The composition on the DGEBA−EBBA side was estimated from the particular $T_{NI}(p)/T_{NI}(p=1)$, read from Figure 7. The resultant ratio was used in Figure 3 to estimate the amount of DGEBA in the EBBA-rich phase. Although this representation constitutes an oversimplified description of the phase separation process, it permits a simple visualization of the evolution of the system along reaction. The diagram is exclusively valid for the selected values of initial composition and reaction temperature.

Morphologies Generated. The evolution of morphologies was followed by TOM in the course of polymerization at 80 °C. Co-continuous structures were generated and remained stable at full conversion. The observed morphology did not change after prolonged periods of storage (several months) at −18 °C or at room temperature. As an example, Figure 10a,b shows transmission optical micrographs obtained at 40 °C without polarizers for the fully cured PDLC. Both phases are co-continuous and exhibit a relatively uniform characteristic size (Figure 10a). After leaching EBBA with 2-propanol (Figure 10b), no collapse of the epoxy network was observed. The resulting material is a glassy epoxy foam with a continuous micropore-network structure. This type of material might have applications in the field of low-dielectric coatings.

Therefore, the strategy used to generate stable co-continuous structures in PDLCs was successful. It consisted of starting with a composition located in the critical range, inducing phase separation by polymerization at $T > T_{NI}$, and selecting conditions to produce gelation soon after the beginning of phase separation. In this way, co-continuous structures, possibly generated by spinodal demixing, could be fixed in the fully cured PDLC.

Conclusions

An experimental verification of the possibility of generating stable co-continuous structures in PDLCs by polymerization-induced phase separation was presented. The strategy was based on selecting an initial concentration in the critical range to promote a liquid−liquid phase separation by spinodal demixing. The resulting primary structure was fixed by gelation of the polymer network that took place soon after the beginning of phase separation. Co-continuous structures may be useful to generate nematic domains with a uniform characteristic size in the wavelength range of visible light. By leaching the LC with an adequate solvent, a polymer network foam with a continuous microporous structure could be generated.

In the course of the study, the application of different experimental techniques led to some interesting findings. Because of the high fraction of LC used to generate a PDLC, the reaction rate should undergo an instantaneous acceleration at the beginning of the phase separation, simply due to the rapid increase in the concentration of the reactants when the LC solvent is phase-separated. (The effect is not compensated by the slower reaction of the polymer fraction segregated with the LC.) Although this effect has been reported for thermoplastic-modified thermosets,[47] it has not been previously used to detect the beginning of phase separation in PDLCs formed by PIPS. It was also established that the residual fraction of LC in the polymer network can be conveniently estimated using the change in the absorbance of a LC characteristic peak between isotropic and nematic states.[24] Methods based on the extrapolation of experimental measurements made on samples containing different LC concentrations should be applied with caution due to the variation of network topology with dilution (fraction of intramolecular cycles, crosslink density, etc.). This affects the swelling capacity of the fully cured network.

Acknowledgment. Funding for this research was provided by CONICET, ANPCyT, and Fundación Antorchas, Argentina.We acknowledge the excellent comments and suggestions received from the three reviewers that significantly improved the original manuscript.

References and Notes

(1) Doane, J. W.; Vaz, N. A.; Wu, B. G.; Zumer, S. *Appl. Phys. Lett.* **1986**, *48*, 269.
(2) Doane, J. W. In *Liquid Crystals: Applications and Uses*; Bahadur, B., Ed.; World Scientific: Singapore, 1991.
(3) Montgomery, G. P.; Smith, G. W.; Vaz, N. A. In *Liquid Crystalline and Mesomorphic Polymers*; Shibaev, V. P., Lam, L., Eds.; Springer: New York, 1994.

(4) Drzaic, P. S. *Liquid Crystal Dispersions*; World Scientific: Singapore, 1995.
(5) Hirai, Y.; Niiyama, S.; Kumai, H.; Gunjima, T. *SPIE* **1990**, *1257*, 2.
(6) Kirov, N.; Fontana, M. P.; Cavatorta, F. *J. Mol. Struct.* **1980**, *59*, 147.
(7) Kirov, N.; Fontana, M. P.; Affanassieva, N. *Mol. Cryst. Liq. Cryst.* **1982**, *89*, 193.
(8) Krestov, A.; Azarova, G. *Mol. Cryst. Liq. Cryst.* **1990**, *192*, 53.
(9) Fouret, R.; Elouatib, A.; Gors, C.; More, M.; Pepy, G.; Rosta, L. *Phase Transitions* **1991**, *33*, 209.
(10) Ogorodnik, K. Z.; Koshelev, S. D. *Sov. Phys. Crystallogr.* **1978**, *23*, 231.
(11) Yasuniwa, M.; Minato, K. *Mol. Cryst. Liq. Cryst.* **1982**, *87*, 97.
(12) Dolganov, V. K.; Gál, M.; Kroó, N.; Rosta, L.; Szabon, J. *Liq. Cryst.* **1987**, *2*, 73.
(13) Kronberg, B.; Bassignana, I.; Patterson, D. *J. Phys. Chem.* **1978**, *82*, 1719.
(14) Kronberg, B.; Bassignana, I.; Patterson, D. *J. Phys. Chem.* **1978**, *82*, 1714.
(15) Dubault, A.; Casagrande, C.; Veyssie, M. *Mol. Cryst. Liq. Cryst.* **1982**, *72*, 189.
(16) Kelkar, V. K.; Manohar, C. *Mol. Cryst. Liq. Cryst.* **1986**, *133*, 267.
(17) Serbutoviez, C.; Kloosterboer, J. G.; Boots, H. M. J.; Touwslager, F. J. *Macromolecules* **1996**, *29*, 7690.
(18) Kloosterboer, J. G.; Serbutoviez, C.; Touwslager, F. J. *Polymer* **1996**, *37*, 5937.
(19) Serbutoviez, C.; Kloosterboer, J. G.; Boots, H. M. J.; Paulissen, F. A. M. A.; Touwslager, F. J. *Liq. Cryst.* **1997**, *22*, 145.
(20) Nwabunma, D.; Kim, K. J.; Lin, Y.; Chien, L. C.; Kyu, T. *Macromolecules* **1998**, *31*, 6806.
(21) Nwabunma, D.; Kyu, T. *Macromolecules* **1999**, *32*, 664.
(22) Bhargava, R.; Wang, S. Q.; Koenig, J. L. *Macromolecules* **1999**, *32*, 2748.
(23) Bhargava, R.; Wang, S. Q.; Koenig, J. L. *Macromolecules* **1999**, *32*, 8982.
(24) Bhargava, R.; Wang, S. Q.; Koenig, J. L. *Macromolecules* **1999**, *32*, 8989.
(25) Lucchetti, L.; Simoni, F. *J. Appl. Phys.* **2000**, *88*, 3934.
(26) Nwabunma, D.; Chiu, H. W.; Kyu, T. *Macromolecules* **2000**, *33*, 1416.
(27) Nwabunma, D.; Kyu, T. *Polymer* **2001**, *42*, 801.
(28) Vázquez, A.; Bentaleb, D.; Williams, R. J. J. *J. Appl. Polym. Sci.* **1991**, *43*, 967.
(29) Rozenberg, B. A. *Adv. Polym. Sci.* **1986**, *75*, 113.
(30) Fedtke, M. *Makromol. Chem. Macromol. Symp.* **1987**, *7*, 153.
(31) Berger, J.; Lohse, F. *Eur. Polym. J.* **1985**, *21*, 435.
(32) Vázquez, A.; Deza, R.; Williams, R. J. J. *Polym. Bull. (Berlin)* **1992**, *28*, 459.
(33) Galante, M. J.; Vázquez, A.; Williams, R. J. J. *Polym. Bull. (Berlin)* **1991**, *27*, 9.
(34) Williams, R. J. J.; Rozenberg, B. A.; Pascault, J. P. *Adv. Polym. Sci.* **1997**, *128*, 95.
(35) Pascault, J. P.; Williams, R. J. J. In *Polymer Blends*; Paul, D. R., Bucknall, C. B., Eds.; Wiley: New York, 2000; Vol. 1, Chapter 13, p 379.
(36) Borrajo, J.; Riccardi, C. C.; Williams, R. J. J.; Masood Siddiqi, H.; Dumon, M.; Pascault, J. P. *Polymer* **1998**, *39*, 845.
(37) St John, N. A.; George, G. A. *Polymer* **1992**, *33*, 2679.
(38) Min, B. G.; Stachurski, Z. H.; Hodgkin, J. H.; Heath, G. R. *Polymer* **1993**, *34*, 3620.
(39) Poisson, N.; Lachenal, G.; Sautereau, H. *Vib. Spectrosc.* **1996**, *12*, 237.
(40) Masood Siddiqi, H.; Dumon, M.; Pascault, J. P. *Mol. Cryst. Liq. Cryst.* **1998**, *312*, 137.
(41) Boots, H. M. J.; Kloosterboer, J. G.; Serbutoviez, C.; Touwslager, F. J. *Macromolecules* **1996**, *29*, 7683.
(42) Colthup, N. B.; Daly, L. H.; Wiberley, S. E. *Introduction to Infrared and Raman Spectroscopy*, 2nd ed.; Academic Press: New York, 1975.
(43) Shaya, S. A.; Yu, H. *J. Phys., Colloq.* **1975**, *36*, C1.
(44) Maier, W.; Saupe, A. *Z. Naturforsch. A* **1959**, *14*, 882.
(45) Maier, W.; Saupe, A. *Z. Naturforsch. A* **1960**, *15*, 287.
(46) Shen, C.; Kyu, T. *J. Chem. Phys.* **1995**, *102*, 556.
(47) Bonnet, A.; Pascault, J. P.; Sautereau, H.; Taha, M.; Camberlin, Y. *Macromolecules* **1999**, *32*, 8517.
(48) Peebles, L. H., Jr. *Molecular Weight Distributions in Polymers*; Wiley-Interscience: New York, 1971.
(49) Riccardi, C. C.; Borrajo, J.; Williams, R. J. J.; Masood Siddiqi, H.; Dumon, M.; Pascault, J. P. *Macromolecules* **1998**, *31*, 1124.
(50) Smith, G. W.; Ventouris, G. M.; West, J. L. *Mol. Cryst. Liq. Cryst.* **1992**, *213*, 11.
(51) Smith, G. W. *Mol. Cryst. Liq. Cryst.* **1994**, *239*, 63.
(52) Fox, T. G. *Bull. Am. Phys. Soc.* **1956**, *1*, 123.

MA0200120